Measurement of the Frequency-Dependent Conductivity in Sapphire

Jie Shan,[1,*] Feng Wang,[1] Ernst Knoesel,[1,†] Mischa Bonn,[2] and Tony F. Heinz[1]

[1]*Departments of Physics and Electrical Engineering, Columbia University, 538 West 120th Street, New York, New York 10027, USA*

[2]*Leiden Institute of Chemistry, P.O. Box 9502, 2300 Leiden, The Netherlands*

(Received 5 March 2003; published 17 June 2003)

Electron transport of photoexcited single-crystal sapphire (α-Al_2O_3) is characterized by terahertz time-domain spectroscopy. The complex conductivity displays a Drude-type frequency dependence, which yields carrier scattering rates and densities. Carrier scattering is dominated by interactions with acoustical and optical phonons at low and high temperatures, respectively, and follows Matthiessen's law over the measured temperature range of 40–350 K. The results, including low-temperature mobilities $> 10\,000$ cm^2/V s, are compatible with a large-polaron description of the conduction electrons.

DOI: 10.1103/PhysRevLett.90.247401 PACS numbers: 78.47.+p, 71.38.–k, 72.10.–d, 72.80.–r

The nature of charge transport in normally insulating solids is a subject of considerable practical and fundamental importance. With respect to the former motivation, charge transport in excited insulators plays a key role in devices as varied as detectors of ionizing radiation and solar cells. Charge transport also controls electrical and optical breakdown phenomena in insulating materials, properties that often define their utility in electronic and laser applications. On the fundamental side, there is inherent interest in being able to examine the properties of charge carriers in materials with wide band gaps, just as has been done comprehensively in metals and semiconductors where mobile charge carriers are already present or may be introduced by doping. Of particular significance is the role of polaronic effects in ionic insulators. Because of the strong interaction between conduction electrons and phonons in such polar materials, charge carriers are surrounded by a cloud of virtual phonons. In the strong coupling limit, this leads to the formation of small polarons and carrier localization through self-trapping. For weaker coupling, the charge carriers form large polarons, quasiparticles that remain mobile but exhibit an enhanced effective mass m^* as they travel through the solid. As an early example of the application of quantum field theory to condensed matter physics [1], this problem has attracted much theoretical attention [1–7] and, accordingly, many models of polaronic transport have been developed under differing approximations.

In view of these diverse motivations, one might expect there to be a large body of reliable experimental data on basic properties of carrier transport in insulators. That this is not the case reflects the experimental challenges in performing such measurements. Unlike metals and semiconductors, charge carriers are typically present only under nonequilibrium conditions. Conventional approaches to examine charge transport processes are further impeded by the difficulty in making electrical contacts to insulators and the short lifetime of the carriers prior to trapping or recombination. One approach to overcome these difficulties is the use of optical pump/probe measurements. Such studies can provide exceptional time resolution and valuable information on the temporal evolution of the carrier energy distribution. They do not generally provide a direct link to transport properties as manifested in the conductivity of the material. From this perspective, terahertz time-domain spectroscopy (THz TDS) [8], combined with ultrafast optical excitation, offers a powerful probe of charge transport and ultrafast carrier dynamics in condensed matter [9,10]. The technique provides an accurate determination of the complex conductivity of the sample over the THz frequency range. The pulsed nature of the THz radiation allows one to probe short-lived carriers and to examine the corresponding temporal evolution of the conductivity.

In this Letter, we describe the application of THz TDS with ultrafast optical pumping to examine charge transport in an insulating solid. As a prototype of a well-characterized material with significant applications in electronics and optics, we have chosen single-crystal sapphire (α-Al_2O_3). Although there has been considerable effort studying this material system [11–14] and there is agreement that electrons dominate charge transport, the reported mobilities at room temperature range from 0.05 [13] to 90 cm^2/V s [14]. The uncertainties reflect complications arising from the short carrier lifetimes, the nature of electrical contacts to sapphire, and the influence of shallow trap states [15]. We report here measurements of the photoinduced high-frequency complex conductivity of sapphire over a broad range of temperatures (40–350 K). We show that this transient conductivity can be adequately described by the Drude model at all temperatures, thus permitting us to extract the electron scattering rate. The temperature dependence of the scattering rate can be understood in terms of contributions from acoustical and longitudinal optical (LO) phonons. A comparison of the experimental findings with large-polaron theories allows us to estimate parameters characterizing electron-phonon interactions, as well as to examine distinctions among the various theoretical models. Our

results show that the electron mobility in high-purity sapphire (with $m^* = 0.30m_0$) can be as high as 600 $cm^2/V\,s$ at room temperature and that the mobility increases sharply with decreasing temperature. At 40 K, the electron mobility exceeds 10 000 $cm^2/V\,s$, a value normally associated with high-mobility semiconductors.

The experimental apparatus and procedure are similar to those used in an earlier measurement [9]. The laser source is an amplified, mode-locked Ti:sapphire system, which provides pulses of approximately 100-fs duration at a wavelength of 810 nm and a repetition rate of 1 kHz. Charge carriers in sapphire, with its band gap of $E_g = 8.7$ eV [16], are created through a two-photon absorption process by the third harmonic of the Ti:sapphire laser. The pump-induced changes of the material are probed by THz pulses introduced at a suitable delay time. The THz probe pulses are generated and detected, respectively, by optical rectification and electro-optic sampling of the femtosecond laser pulses in ZnTe crystals. The sapphire sample was a high-purity substrate (impurity level <30 ppm) of 0.5 mm thickness. Most of the experiments were carried out with the THz electric field perpendicular to the c axis of the sapphire crystal.

In the measurements, we recorded the electric-field waveform $E(t)$ of THz pulses transmitted through the unexcited sapphire crystal and the pump-induced change in the THz waveform, $\Delta E(t)$. A delay of several picoseconds after pump excitation was chosen to ensure that any hot carrier effects had abated, but that carrier density had not decreased significantly. Figure 1 illustrates representative waveforms of $E(t)$ and $\Delta E(t)$ measured for the sample at room temperature. We extracted the pump-induced complex conductivity, $\sigma(\nu) = \sigma'(\nu) + i\sigma''(\nu)$, as a function of the frequency ν through Fourier transformation of the recorded waveform of $E(t)$ and $\Delta E(t)$. The analysis was performed within an approximation of quasi-steady-state material response according to the procedure presented previously in [9].

The corresponding frequency-dependent conductivity, $\sigma(\nu) = \sigma'(\nu) + i\sigma''(\nu)$, is shown in Fig. 2. The experimental results (dots) are found to be compatible with simple Drude behavior of $\sigma(\nu) = \omega_p^2/(\gamma_o - i2\pi\nu)$, shown as solid lines. Here γ_0 denotes the electron scattering rate, and $\omega_p = [ne^2/(\varepsilon_0 m^*)]^{1/2}$ is the plasma frequency, which is related to the electron effective mass (m^*), the density of conduction electrons (n), and the permittivity of free space (ε_0). The fit to the Drude model (solid lines in Figs. 1 and 2) is satisfactory, particularly given the fact that the single adjustable parameter γ_0 determines both the shape and relative amplitude of the two functions $\sigma'(\nu)$ and $\sigma''(\nu)$. The corresponding fit to the time-domain data is shown in Fig. 1. We note that to experimental accuracy, there appears to be no need to include the hole contribution to the conductivity, as expected from previous x-ray and Hall studies [11–14], as well as from the large predicted hole mass [17]. From the fitting procedure, we obtain a room-temperature scattering rate of $\gamma_0 = (95\ \text{fs})^{-1}$ and a plasma frequency of $\omega_p = 2\pi \times 0.15$ THz. These parameters are similar for the THz electric field both perpendicular and parallel to the c axis, and we conclude that the possible anisotropy in the conductivity tensor of sapphire is modest. In an earlier THz measurement by Haran *et al.* [18] under different excitation conditions, changes in the THz transmission in sapphire were also observed but were ascribed to the contribution of phonons.

We have further investigated the nature of the charge transport by examining the dependence of the conductivity on carrier density and sample temperature. The carrier density can be controlled experimentally by varying the pump fluence. A quadratic variation of the carrier density with pump fluence was observed, as expected for a two-photon excitation process. Beyond this effect, however, the conductivity remained Drude-like in form and showed no significant variation of the scattering rate with carrier density. This indicates that

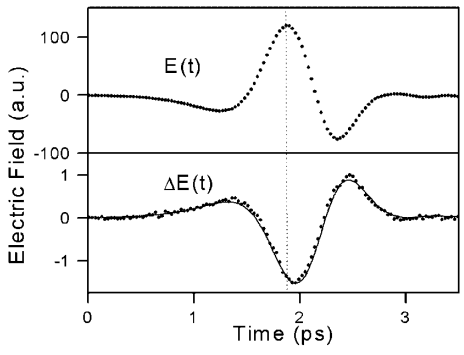

FIG. 1. Top panel: the transmitted THz electric-field waveform $E(t)$ in sapphire; Bottom panel: pump-induced change in the THz waveform $\Delta E(t)$ (dots) at room temperature and a fit to the Drude model (solid curve). The pump fluence was 3 J/m^2 and the pump-probe time delay was 5 ps.

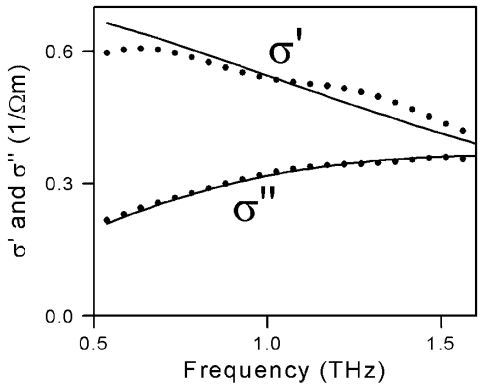

FIG. 2. Frequency dependence of the real (σ') and the imaginary part (σ'') of the pump-induced complex conductivity (dots) of sapphire at room temperature. The solid curves represent a fit to the Drude model.

carrier-carrier scattering is negligible under the experimental excitation conditions, as expected for the relatively low carrier concentrations of $n \sim 10^{12}$–10^{14} cm^{-3} under consideration.

With decreasing sample temperature the conductivity also retained its Drude form, but exhibited a sharply reduced scattering rate. As shown in Fig. 3, the scattering rate drops from $\gamma_0 = (95\ \text{fs})^{-1}$ at room temperature to $\gamma_0 = (5\ \text{ps})^{-1}$ at 40 K, a decrease by a factor of ~50. An examination of the temperature dependence of γ_0 reveals an activated behavior at high temperatures ($T > 200$ K) and a weaker variation at low temperatures ($T < 200$ K). These features are characteristic of LO-phonon and acoustic phonon scattering, respectively. To describe the total scattering rate, we sum over all phonon modes using Mathiessen's law [19]:

$$\gamma_0 = \gamma_{ac}(T) + \sum_s \gamma^s_{\text{LO}}(T) + \gamma_{\text{imp}}(T), \tag{1}$$

where γ_{ac} and $\sum \gamma^s_{\text{LO}}$ are, respectively, the scattering rates from acoustic phonons and the sum of all LO-phonon modes. In Eq. (1) we have also included a term γ_{imp} representing scattering from impurities and defects, which was found to be negligible for high-purity samples in our temperature range.

Under the effective mass approximation, the acoustic phonon scattering rate is [20]

$$\gamma_{ac}(T) = \frac{3\varepsilon^2_{\text{def}} m^{*3/2}}{2(2\pi)^{1/2} c_{ii} \hbar^4} (kT)^{3/2}. \tag{2}$$

In this expression, m^* is the effective or polaron mass of the electron, which includes both the effect of the band structure and the mass enhancement from electron interaction with LO phonons. $c_{ii} \approx 5 \times 10^{12}$ dyn/cm^2 [21] denotes the elastic constant, and ε_{def} denotes the electron deformation potential. This latter quantity, defined as the energy shift of the conduction band per unit dilation, is a good measure of the electron-acoustic phonon coupling. Neither m^* nor ε_{def} has been previously measured in sapphire.

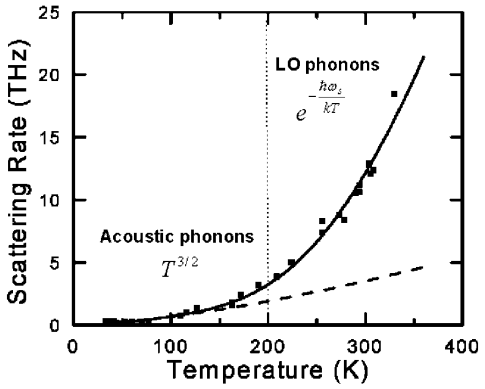

FIG. 3. Temperature dependence of the scattering rate in high-purity sapphire (squares). The solid line is a fit to a transport model that includes LO-phonon and acoustic phonon scattering, as described in the text. The dashed line shows the acoustic phonon contribution. At the temperatures above that denoted by the dotted line, LO-phonon scattering dominates.

As for the LO-phonon scattering, we use the results of Low and Pines [2]:

$$\gamma^s_{\text{LO}} = \left(\frac{m^*}{m}\right)^2 \frac{2\alpha_s \omega_s}{f(\alpha_s)} e^{-\hbar\omega_s/kT}. \tag{3}$$

Here m is the electron band mass, ω_s is the frequency of the LO phonon of mode s, and α_s is the corresponding dimensionless electron-LO phonon coupling parameter. For moderate coupling ($\alpha_s < 6$), the polaron mass m^* and the electron band mass m are related by $m^* = (1 + \Sigma_s \alpha_s/6)m$, and $f(\alpha_s) \approx 1$. The LO-phonon frequencies and their coupling to electrons can be obtained from analysis of infrared spectra, since they determine the dielectric function of the material $\varepsilon(\omega)$ [22]:

$$\frac{1}{\varepsilon(\infty)} - \frac{1}{\varepsilon(\omega)} = \sum_s \alpha_s \frac{\hbar}{e^2} \left(\frac{2\hbar\omega_s}{m}\right)^{1/2} \frac{\omega_s^2}{\omega_s^2 - \omega^2}. \tag{4}$$

From the infrared spectra of Schubert *et al.* [23], we obtained the values for ω_s and $\alpha_s/(m/m_0)^{1/2}$ indicated in Table I. Several observations may be made with reference to Table I. First, given the values of the coupling strength $\alpha_s/(m/m_0)^{1/2}$ and assuming that the band mass m does not substantially exceed the free electron mass m_0 [17], we are indeed in the limit of large polarons ($\alpha_s < 6$). Second, for each of the two distinct crystallographic directions ($\parallel$ or $\perp$ to the c axis), there is just one dominant phonon mode with $\hbar\omega_s \approx 110$ meV $\approx k_B$ 1280 K. Given the relatively high energy of these modes, this interaction will be frozen out in the lower temperature range, in accordance with Fig. 3. Third, since the energies and couplings of the dominant phonon modes are similar along both directions, we would not expect strong anisotropy in the conductivity, in accordance with the experimental observations described above.

By combining Eqs. (1)–(3) and using the values for ω_s and $\alpha_s/(m/m_0)^{1/2}$ from Table I, we are able to reproduce the temperature dependence of the scattering rate quite satisfactorily, as indicated in Fig. 3. The fit involves just two free parameters: the deformation potential, ε_{def}, and the electron band mass, m. We obtain $\varepsilon_{\text{def}} = 19$ eV and $m = 0.25m_0$ (or, equivalently, $m^* = 0.3m_0$). These values are in fair agreement with the theoretical values from total-energy [24] and band structure [17] calculations. If we examine other theories of charge transport by large

TABLE I. Electron-optical phonon coupling parameters for different LO phonon modes of sapphire as deduced from the infrared transmission data of Schubert *et al.* [23].

LO phonon	E_u ($E \parallel c$ axis)		A_{2u} ($E \perp c$ axis)			
$\hbar\omega_s$ (meV)	109	63.3	112	78.1	59.7	48
$\alpha_s/(m/m_0)^{1/2}$	2.05	0.28	2.29	0.012	0.136	0.034

polarons, we generally find the same exponential temperature dependence from thermal excitation of optical phonons. Most models are thus compatible with the experimental shape of $\gamma_0(T)$. The fits require, however, quite different values for the deformation potential and electron band mass m. For example, the models of Kadanoff [6] and Garcia-Moliner [5] require, respectively, values of $\varepsilon_{\text{def}} = 13$ and 14 eV, and $m = 0.44m_0$ and $0.38m_0$. It would be desirable to have an independent experimental determination of the electron mass (such as a cyclotron resonance measurement), which would allow a definite conclusion about the accuracy of different polaron transport models.

It is also appropriate to add a few words about the Drude-like form of the frequency-dependent conductivity $\sigma(\nu)$ that has been measured experimentally. Given the strong electron-phonon interactions in our system, is this simple result compatible with theoretical expectations for transport by large polarons? In fact, within the quasiparticle picture of polarons, the dressed electrons are scattered only by *residual* interactions with thermally excited phonons; they behave much like conventional carriers in a solid, but with a renormalized mass of m^*. While this description clearly breaks down when the system is probed at frequencies approaching those of the dressing LO phonons, at lower frequencies we would expect $\sigma(\nu)$ to show the Drude-like behavior generally exhibited by band electrons. The frequency dependence of polaronic conductivity has in fact been considered explicitly in variational calculations of polaron transport by Feynman *et al.* [7]. In the experimentally relevant limit of low frequency and low temperature compared to the optical phonon frequency, the observed Drude conductivity is indeed predicted.

The scattering rate γ_0 also determines the electron mobility μ_e through the relation $\mu_e = e/(m^*\gamma_0)$. To evaluate this expression, we use the effective mass of $m^* = 0.3m_0$ inferred above. At room temperature, we obtain $\mu_e \approx 600\ \text{cm}^2/\text{V s}$. At lower temperatures, μ_e rises rapidly, reaching as high as $30\,000\ \text{cm}^2/\text{V s}$ at 40 K. This sharp increase reflects the complete freezing out of the LO phonons and the reduced interaction with acoustic phonons. Mobilities in this range are commonly associated with high-purity semiconductors, but, as is clear from the discussion above, can also be expected in wide-gap materials having sufficiently low defect densities.

In summary, we have measured the frequency-dependent complex conductivity of electrons in sapphire over a temperature range of 40–300 K by means of THz time-domain spectroscopy. The frequency dependence of the conductivity is found to correspond to that predicted by the Drude model. The temperature dependence of the inferred scattering rates agrees with Matthiessen's law and is compatible with large-polaron theory, particularly that of Low and Pines [2]. While the specific results reported here reflect the properties of sapphire, both the experimental method of THz TDS and the conclusion of the possibility of achieving high carrier mobilities at low temperatures should be broadly applicable to other wide-gap crystalline solids.

The authors thank Dr. J. C. Boettger for providing unpublished results. This work was supported primarily by the Nanoscale Science and Engineering Initiative of the National Science Foundation under NSF Award No. CHE-0117752.

*Current address: Department of Physics, Case Western Reserve University, 10900 Euclid Avenue, Cleveland, OH 44106, USA.

†Current address: Department of Physics and Astronomy, Rowan University, 201 Mullica Hill Road, Glassboro, NJ 08028, USA.

[1] H. Fröhlich, H. Pelzer, and S. Zienau, Philos. Mag. **41**, 221 (1950); H. Fröhlich, Adv. Phys. **3**, 325 (1954).
[2] F. E. Low and D. Pines, Phys. Rev. **98**, 414 (1955).
[3] T. D. Schultz, Phys. Rev. **116**, 526 (1959).
[4] Y. Osaka, Prog. Theor. Phys. **25**, 517 (1961).
[5] F. Garcia-Moliner, Phys. Rev. **130**, 2290 (1963).
[6] L. P. Kadanoff, Phys. Rev. **130**, 1364 (1963).
[7] R. P. Feynman, R. W. Hellwarth, C. K. Iddings, and P. M. Platzman, Phys. Rev. **127**, 1004 (1962).
[8] D. R. Grischkowsky, in *Frontiers in Nonlinear Optics*, edited by H. Walther, N. Koroteev, and M. O. Scully (Institute of Physics, Philadelphia, 1993).
[9] E. Knoesel, M. Bonn, J. Shan, and T. F. Heinz, Phys. Rev. Lett. **86**, 340 (2001).
[10] For recent applications, see, for example, M. C. Beard, G. M. Turner, and C. A. Schmuttenmaer, J. Phys. Chem. B **106**, 7146 (2002); R. D. Averitt *et al.*, Phys. Rev. Lett. **87**, 017401 (2001); F. A. Hegmann *et al.*, Phys. Rev. Lett. **89**, 227403 (2002), and references therein.
[11] R. C. Hughes, Phys. Rev. B **19**, 5318 (1979).
[12] P. S. Pickard and M. V. Davis, J. Appl. Phys. **41**, 2636 (1970).
[13] U. E. Hochuli, Phys. Rev. **133**, A468 (1964).
[14] B. A. Green and M. V. Davis, Trans. Am. Nucl. Soc. **16**, 75 (1973).
[15] R. W. Klaffky, B. H. Rose, A. N. Goland, and G. J. Dienes, Phys. Rev. B **21**, 3610 (1980).
[16] J. Olivier and R. Poirier, Surf. Sci. **105**, 347 (1981).
[17] Y. N. Xu and W. Y. Ching, Phys. Rev. B **43**, 4461 (1991).
[18] G. Haran, W. Sun, K. Wynne, and R. M. Hochstrasser, Chem. Phys. Lett. **274**, 365 (1997).
[19] N. W. Ashcroft and N. D. Mermin, *Solid State Physics* (Saunders College, Philadelphia, 1976).
[20] J. Bardeen and W. Shockley, Phys. Rev. **80**, 72 (1950).
[21] *American Institute of Physics Handbook* (McGraw-Hill, New York, 1972), 3rd ed.
[22] Y. Toyozawa, in *Polarons in Ionic Crystals and Polar Semiconductors*, edited by J. T. Devreese (Elsevier, New York, 1972).
[23] M. Schubert, T. E. Tiwald, and C. M. Herzinger, Phys. Rev. B **61**, 8187 (2000).
[24] J. C. Boettger, Phys. Rev. B **55**, 750 (1997); (private communication).